

RESEARCH PAPER

Cytotoxicity effects of synthesized ZnO and Zn_{0.97}X_{0.03}O (X=Li, Na, and K) nanoparticles by the gelatin-based sol-gel method

Ali Khorsand Zak*

Nanotechnology Laboratory, Esfarayen University of Technology, Esfarayen, North Khorasan, Iran

ABSTRACT

Objective: In this study we would like to report the synthesis of pure and group I element doping of ZnO nanoparticles (ZnO-NPs) prepared using gelatin. The use of natural polymers for the preparation of the pure and doped nanoparticles can result in achieving low cost and eco-friendly advantages.

Materials and Method: Pure and doped ZnO-NPs were obtained at 500 °C and The cytotoxicity of nanoparticles was evaluated using 3-(4,5-dimethylthiazol-2-yl)-2,5-diphenyltetrazolium bromide (MTT) assay. Briefly, neuro2A cells were seeded at a density of 1×10^4 cells per well in 96-well plates and incubated for 24h. Thereafter, the cells were treated with various concentrations of nanoparticles in the presence of 10% FBS.

Results: X-ray diffraction (XRD) analysis revealed wurtzite hexagonal structure for the prepared nanoparticles. No other peaks related to the other compounds are detected which indicate that the doped group one elements have been diffused into ZnO lattice. Field emission scanning electron microscopy (FESEM) showed that the formation of most nanoparticles in nano scale. In vitro cytotoxicity studies on neuro2A cells show the non-toxic effect of concentration below ~250 µg/mL for pure and K doped ZnO-NPs and ~63 µg/mL for Li and Na doped ZnO-NPs. Conclusion: The results show that the potentials of the prepared doped samples to be used in cancer treatments.

Keywords: ZnO; Cytotoxicity; Zinc oxide; Doping

How to cite this article

Khorsand Zak A. Cytotoxicity effects of synthesized ZnO and Zn_{0.97}X_{0.03}O (X=Li, Na, and K) nanoparticles by the gelatin-based sol-gel method. *Nanomed J.* 2017; 4(3): 170-176. DOI: [10.22038/nmj.2017.8958](https://doi.org/10.22038/nmj.2017.8958)

INTRODUCTION

Due to their interesting properties, ZnO nanoparticles (ZnO-NPs) are known as important inorganic semiconductor materials. Therefore, they have wide applications in various fields including catalysis [1], pigments [2], chemical sensors [3], medical treatments [4], and skin care [5]. Doping elements in ZnO matrix is known as a way to control and change its properties. Numerous studies have been carried out to study the physical, chemical, and medical properties of ZnO-NPs doped by several elements [6-10]. Also, it has been found that ZnO particles in nano-size possess unique properties. Therefore, several reports are provided on the synthesis of pure and doped ZnO-NPs such as sol-gel [11], solvo- and hydrothermal [12, 13], precipitations [14], sono-chemical [15], and CVD and VLS [6, 16].

The preparation method is chosen based on the type of application required. Among the above mentioned methods, sol-gel has gained lots of interest since it is a low cost and simple method. Recently, biomaterials, such as natural materials like gelatin, chitosan, and starch [18-20], have been used for the preparation of ZnO-NPs using sol-gel method. Gelatin found to be a suitable biomaterial extracted from the partial hydrolysis of collagen which has good bio-compatibility [17].

The cytotoxicity and antibacterial properties of nanoparticles is a big issue which must be taken into account in medical applications of these materials [18-21].

Many parameters have been identified as being effective in nanomaterial toxicity. Therefore, it seems to be crucial to determine the cytotoxicity of each nanomaterial specifically [22]. Moreover, due to the different in the experimental it is difficult to compare their cytotoxicity results [23]. ZnO has a lot of medical applications due to its interesting

* Corresponding Author Email: alikhorsandzak@gmail.com
Note. This manuscript was submitted on April 10, 2017; approved on June 15, 2017

biological properties, Because doped ZnO-NPs have some medical applications, we evaluate the cytotoxicity of the prepared NPs to gain a better insight into the biological effect of ZnO-NPs. As mentioned earlier, pure and doped ZnO-NPs are present in several materials used for medical applications such as skin UV protection creams. So, investigations are carried out on the cytotoxicity of ZnO-NPs with different morphologies and sizes [24]. The study of the safety issues of this material on humans and environment is significantly important. Many invitro studies show that a small amount of ZnO-NPs reduces cell viability from 100% to almost zero. The even can be attributed to free intracellular Zn^{2+} from dissolving of ZnO-NPs [25]. As an example, the inhalation of ZnO-NPs (20nm, 2.5 mg/Kg, bw) twice daily amount results in an increase in Zn^{2+} content in the liver and kidneys and causes damage in liver and lung tissues according to histopathology results [26].

In this study, $Zn_{0.97}X_{0.03}O$ (X= Li, Na, and K) nanoparticles were fabricated using sol-gel method and gelatin as stabilizing agent. The complex structure of gelatin enables it to stabilize zinc species and nano-particles while inhibiting their excessive aggregation or crystal growth. Also, the cytotoxic effect of the nanoparticles on neuro2A cells was examined.

MATERIALS AND METHODS

All the materials used were of analytical grade and were used without any purification. To synthesize $Zn_{0.97}X_{0.03}O$ (X=Li, Na, and K) nanoparticles, analytical-grade Zinc nitrate hexahydrate ($Zn(NO_3)_2 \cdot 6H_2O$ purchased from Merk), lithium nitrate ($LiNO_3$ purchased from Merk) sodium nitrate ($NaNO_3$ purchased from Merk), and potassium nitrate (KNO_3 purchased from Merk) were used as starting materials. Gelatin [$(NHCOCH-R_1)_n$, R_1 = amino acid purchased from Sigma-Aldrich] and distilled water were used as polymerization agent and solvent, respectively.

Synthesis of ZnO-NPs

The specific amounts of the starting materials were measured to prepare 2 grams of the final product. First, a gelatin solution was prepared by dissolving 8g gelatin in 300 ml distilled water at 60 °C in oil-bath. The appropriate amounts of the nitrates were completely dissolved in 25 ml distilled water. Afterwards, based on the final composition, the needed nitrate solutions

were separately added to the gelatin solution. Meanwhile, the gelatin solution was stirred at 80 °C. A honey wish gels were obtained after about 4 h. The inner wall of the crucible was covered with the obtained gel and then the crucible was placed into the furnace. The temperature of the furnace was fixed at 500°C for 2 h with the heating rate of 2 °C/min. Finally, white and very soft powders were obtained for undoped and doped ZnO-NPs. The same processes were followed to obtain the other compounds.

Characterizations

In order to find out the lowest required calcination temperature, the prepared gel was analyzed using thermogravimetric analyzer (TGA-60/60, Shimadzu). The crystal morphology and the structure of the products were investigated through scanning electron microscopy (SEM, Hitachi H-7100) and X-ray diffraction (XRD, Siemens D5000), respectively.

The evaluation of cytotoxicity effect

The cytotoxicity of nano-particles was evaluated using 3-(4,5-dimethylthiazol-2-yl)-

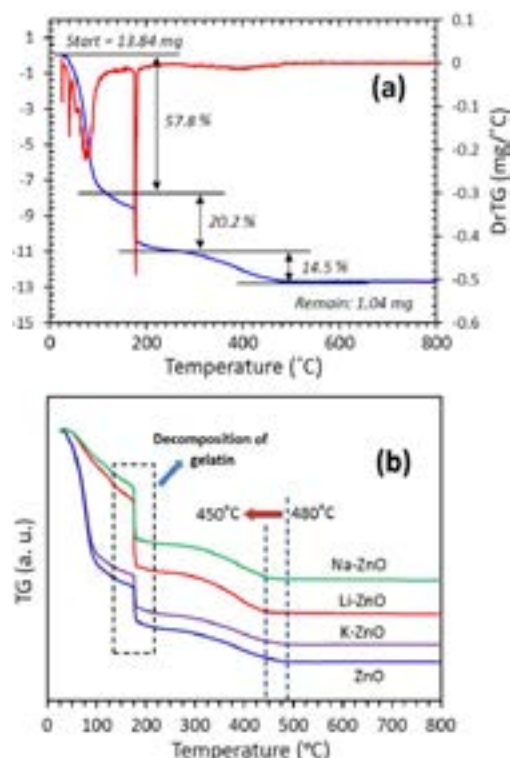


Fig. 1. (a) Thermogravimetric and the corresponding first derivative of pure ZnO gel. (b) thermogravimetric analysis of pure and doped ZnO gels

2,5-diphenylte-trazolium bromide (MTT) assay [27]. Briefly, neuro2A cells were seeded at a density of 1×10^4 cells per well in 96-well plates and incubated for 24 h. Thereafter, the cells were treated with various concentrations of nanoparticles in the presence of 10% FBS. The ZnO-NPs calcined at 600 °C were suspended in a stock solution at 5 $\mu\text{g}/\text{ml}$ in a solution of dimethylsulfoxide (DMSO)/double distilled water. After 24 h of incubation, 20 μl of 5mg/ml MTT in the PBS buffer was added to each well, and the cells were further incubated for 4 h at 37 °C. The medium containing unreacted dye was discarded, and 100 μl of DMSO was added to dissolve the formazan crystal formed by live cells. Optical absorbance was measured at 590nm (reference wavelength 630 nm) using a micro-plate reader (Statfax-2100, A wareness Technology, USA), and cell viability was expressed as a percent relative to untreated control cells. Values of metabolic activity are presented as mean \pm SD of triplicates [28].

RESULTS

Thermogravimetric and the first derivative analysis (TGA/DrTG) curves of the prepared pure ZnO gel precursor by sol-gel method using gelatin are presented in Fig 1a.

The heating process was started from the room temperature up to 800 °C along with a temperature rate of 5 °C/min. The TGA curve descends until getting horizontal at about 480 °C and weight loss of 92.5% was observed during the heating process. Three main regions are detected in TGA curve.

XRD patterns of the prepared pure ZnO and $\text{Zn}_{0.97}\text{X}_{0.03}\text{O}$ (X=Li, Na, and K) NPs in the range of

$2\theta = 20\text{--}70^\circ$ are shown in Fig 2. All detectable peaks with Miller indexes (100), (002), (101), (102), (103), (200), (112), (201), and (004) can be indexed to the ZnO wurtzite structure (PDF card no: 00–005–0664). No further peaks were detected related to Na, K, Na_2O , K_2O , Li_2O and other similar compounds. There was also an increase in (101) diffraction peak intensity for ZnO samples doped by Li, Na and K elements compared to the undoped ZnO-NPs shown in Fig 3.

Wurtzite lattice parameters such as the values of d , the distance between adjacent planes in the Miller indices (hkl) (obtained from the Bragg equation, $\lambda = 2d \sin\theta$), lattice constants a , b , and c , inter-planar angle (the angle ϕ between the planes $(h_1k_1l_1)$, of spacing d_1 and the plane $(h_2k_2l_2)$ of spacing d_2), and unit cell volumes were obtained from the Lattice Geometry equation [26]. The lattice parameters of the samples are summarized in Table 1. The crystallite sizes of the undoped and doped ZnO-NPs were determined by means of a X-ray line-broadening method using the Scherrer equation: $D = (k\lambda/\beta_{\text{hkl}} \cos\theta)$, where D is the crystallite size in nanometers, λ is the wavelength of the radiation (1.54056 Å for CuK_α radiation), k is a constant equal to 0.94, β_{hkl} is the peak width at half-maximum intensity (FWHM), and θ is the peak position. The plane (103) was chosen to calculate the crystallite size, either plane can be used for this purpose. The crystallite sizes of the undoped, K-, Na-, and Li-doped ZnO-NPs were found to be 38 ± 2 , 43 ± 2 , 45 ± 2 , and 48 ± 2 nm, respectively.

Morphology and the related particle size distributions of the undoped, Li-, Na-, and K-doped ZnO-NPs are shown in Figs. 4 (a-d). The results show an average particle size for undoped Li-,

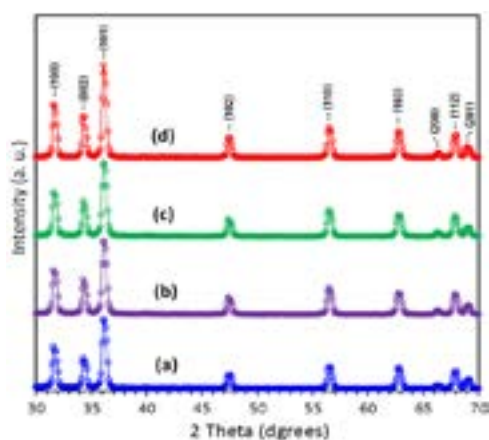


Fig. 2. XRD patterns of (a) pure ZnO-NPs, (b) $\text{Zn}_{0.97}\text{K}_{0.03}\text{O}$, (c) $\text{Zn}_{0.97}\text{Na}_{0.03}\text{O}$, (d) $\text{Zn}_{0.97}\text{Li}_{0.03}\text{O}$

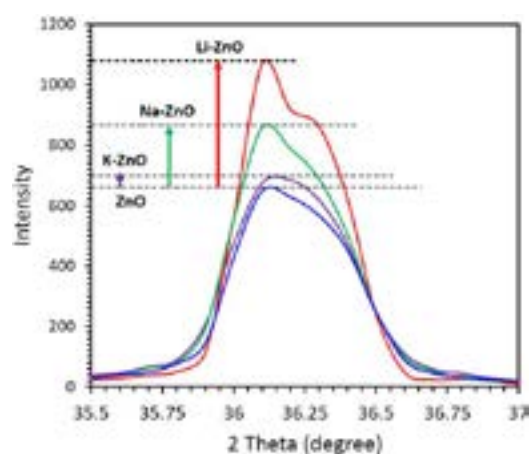


Fig. 3. XRD peak from (101) plans for pure and doped ZnO-NPs

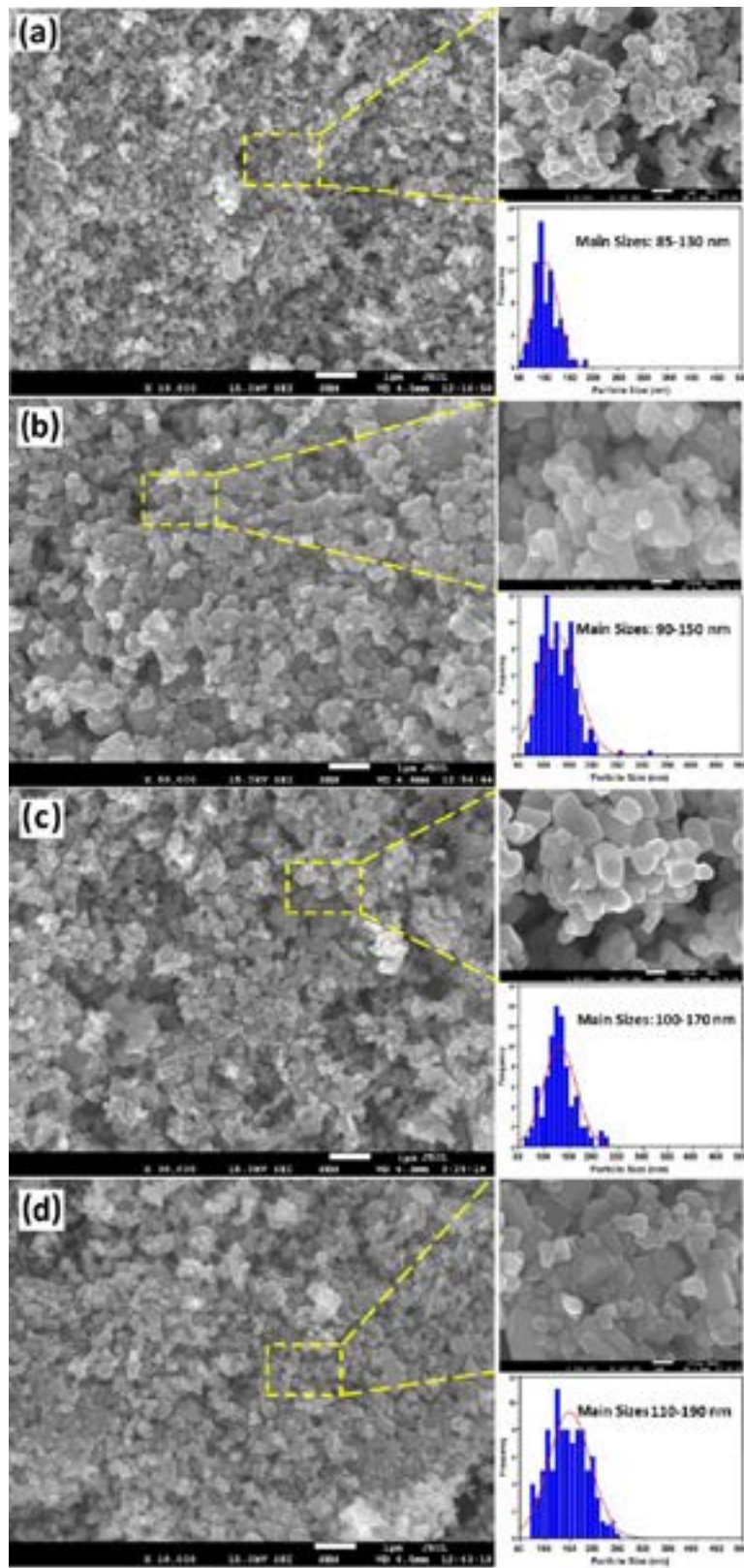


Fig. 4. FESEM micrograph of (a) pure ZnO-NPs, (b) Zn_{0.97}K_{0.03}O, (c) Zn_{0.97}Na_{0.03}O, (d) Zn_{0.97}Li_{0.03}O

Table 1. Lattice parameters of pure and doped ZnO-NPs prepared at different 500 °C. (The measurements were done based on the data obtained at room temperatures of 25 °C)

Compound	2θ ± 0.01	hkl	$d_{hkl}(nm)$ ± 0.0005	Structure	Lattice parameter (nm) ± 0.0005
Zn O	31.71	(100)	0.2821	Hexagonal	a=0.324
	34.37	(002)	0.2608		c/a=1.62
$Zn_{0.97}Li_{0.03}O$	31.71	(100)	0.2821	Hexagonal	a=0.325
	34.38	(002)	0.2607		c/a=1.61
$Zn_{0.97}Na_{0.03}O$	31.71	(100)	0.2821	Hexagonal	a=0.325
	34.35	(002)	0.2610		c/a=1.6
$Zn_{0.97}K_{0.03}O$	31.71	(100)	0.2820	Hexagonal	a=0.325
	34.38	(002)	0.2608		c/a=1.61

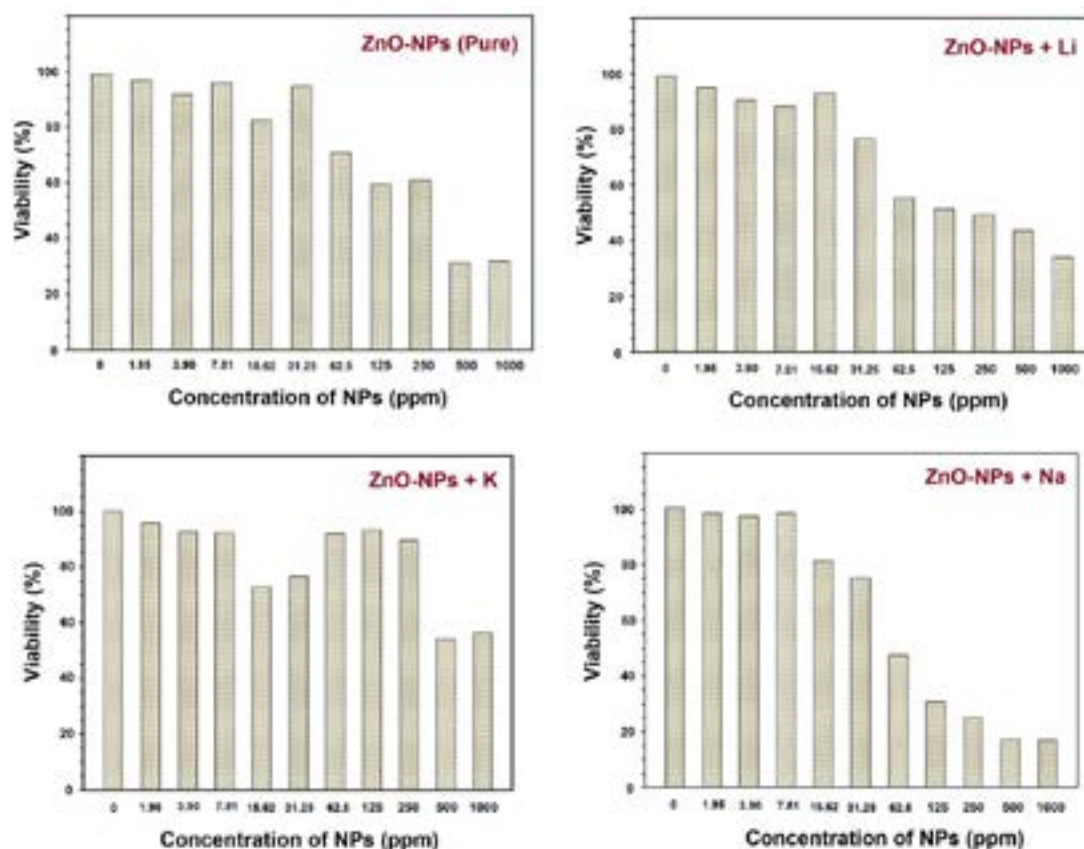


Fig. 5. Cell viability of neuro 2A cells measured by the MTT assay for pure and doped ZnO-NPs

Na-, and K-doped ZnO-NPs about 95±25, 120±30, 135±35, and 150±40 nm, respectively. The results are in good agreement with the TGA results mentioned earlier.

nanopowders, ranging from 0 to 1000 µg/mL, are shown in Fig 5. The pure and K-doped ZnO-NPs samples demonstrated no significant toxicity even in concentrations up to 250 mg/mL in the MTT assay meaning that the prepared nanoparticles are well-tolerated by Neuro2A cells. Whereas, the results showed, in Li and Na -doped ZnO-NPs samples for concentrations above 31µg/

mL, the metabolic activity was decreased. In a concentration dependent manner meaning that the metabolic activity started to decrease from 31µg/mL and reached its maximal decreasing in 500 µg/mL for pure, K, and Na -doped ZnO-NPs and 1000 µg/mL for Li-doped ZnO-NPs.

DISCUSSION

In Fig 1a, the first weight loss Ed1 between the room temperature and 140 °C (57.8%) is related to an initial loss of water. The second weight loss Ed2 occurred between 140 °C and 240 °C with a

weight loss of 20.2% which can be attributed to the decomposition of the aromatic bonds and chemical groups of gelatin. Ed3 which is related to the decomposition of the pyrocholor phases and the formation of ZnO pure phase occurred from 240 to 480 °C (14.5%). There was no further weight loss after 480 °C which indicates the formation of ZnO-NPs above this temperature. Therefore, the temperature of 500 °C was chosen as the calcination temperature for preparing the nanoparticles. The TGA curves of as-prepared gels precursor related to the pure, Li-, Na-, and K-doped ZnO nanoparticles are presented in Fig 1b. It is observed that the weight loss traces are almost the same but the dopants decrease the needed calcination temperature to 450, 460, and 480 °C for Li-, Na-, and K-doped ZnO gel precursor, respectively. This phenomena can be attributed to the high chemical reactivity energy of the group-I elements of the periodic table, which allow them to affect it as a catalyst resulted in an increase in the chemical reactions speed during the calcination process. This effect will be observed in the XRD and SEM results.

According to the XRD results, the crystallite size was increased by doping Li, K, and Na into ZnO. This can be related to charge density of the Li^+ , K^+ , and Na^+ , which help the crystal to grow faster due to their higher chemical reactivity in comparison with Zn^{2+} . The results are in good agreement with the TGA results.

From SEM images, it is clear that Li-doped ZnO nano-particles are bigger compared to the other samples and some of the particles found in hexagonal rod shape as seen in Fig 4d. It can be clearly observed that the nano-particles grew as the ionic radius of doping material increased. It is also observed that the undoped ZnO-NPs, as shown in Fig4a, have uniform distribution of size compared to Li-, Na- and K-doped ZnO-NPs. This poly-disparity of Li-, Na- and K-doped ZnO-NPs can be also due to bigger ionic radii of the Li^+ , Na^+ and K^+ in comparison with ionic radius of the Zn^{2+} .

It has been reported that there is a relationship between cytotoxicity and physicochemical properties of ZnO-NPs such as particle size and surface charge [29].

It was found that the smaller ZnO particles show higher cytotoxic effects compared to larger particles and also the shape of the particles plays an important role in these properties [30, 31]. In addition, some studies report that the cytotoxic

effect of ZnO-NPs also depends upon pH triggered intercellular release of Zn ions and the proliferation rate of mammalian cells [32-35].

The above mentioned studies also found a significant reduction in the viability detected by the MTT assay.

In the study, higher concentrations showed higher response. Therefore, the doped ZnO-NPs for their implications can be used in cancer therapy [36].

CONCLUSION

Pure and group-I element doped ZnO-NPs were synthesized by the sol-gel method using gelatin as a bio-polymeric agent. XRD results showed that all of nanoparticles calcined at 500 °C exhibited high purity with hexagonal (wurtzite) structure. The crystallite size range of 38 to 48 nm and particle size range of 95 to 150 nm were obtained for the pure and doped ZnO-NPs. Based on the above mentioned and the results for cytotoxicity, it can be concluded that this is an interesting synthesis method in which the green chemistry rule is applied and extended in the preparation of pure and doped nanoparticles without special physical conditions. These nanoparticles could be used in different fields such as optical and medical applications.

ACKNOWLEDGMENTS

Author appreciate Esfarayen University of Technology for support this project.

CONFLICT OF INTEREST

Author has no received research grants. The author declares that he has no conflict of interest.

REFERENCES

1. Hong J, He Y. Polyvinylidene fluoride ultrafiltration membrane blended with nano-ZnO particle for photo-catalysis self-cleaning. *Desalination*. 2014; 332(1): 67-75.
2. Soumya S, Mohamed AP, Mohan K, Ananthakumar S. Enhanced near-infrared reflectance and functional characteristics of Al-doped ZnO nano-pigments embedded PMMA coatings. *Sol Energy Mater Sol Cells*. 2015; 143: 335-346.
3. Vanalakar SA, Patil VL, Harale NS, Vhanalakar SA, Gang MG, Kim JY, Patil PS, Kim JH. Controlled growth of ZnO nanorod arrays via wet chemical route for NO₂ gas sensor applications. *Sensors and Actuators B: Chemical*. 2015; 221: 1195-1201.
4. Petkova P, Francesko A, Perelshtein I, Gedanken A, Tzanov T. Simultaneous sonochemical-enzymatic coating of medical textiles with antibacterial ZnO nanoparticles. *Ultrason Sonochem*. 2016; 29: 244-250.
5. Yin H, Casey PS. ZnO nanorod composite with quenched

- photoactivity for UV protection application. *Mater Lett.* 2014; 121: 8-11.
6. Yousefi R, Muhamad MR, Zak AK. Investigation of indium oxide as a self-catalyst in ZnO/ZnInO heterostructure nanowires growth. *Thin Solid Films.* 2010; 518(21): 5971-7.
 7. Yousefi R, Zak AK, Jamali-Sheini F. Growth, X-ray peak broadening studies, and optical properties of Mg-doped ZnO nanoparticles. *Mater Sci Semicond Process.* 2013; 16(3): 771-777.
 8. Yousefi R, Zak AK, Mahmoudian M. Growth and characterization of Cl-doped ZnO hexagonal nanodisks. *J Solid State Chem.* 2011; 184(10): 2678-2682.
 9. Zak AK, Huang NM. Optical properties of group-I-doped ZnO nanowires. *Ceram Int.* 2014; 40: 4327-4332.
 10. Zak AK, Majid WA, Abrishami ME, Yousefi R, Parvizi R. Synthesis, magnetic properties and X-ray analysis of ZnO. 97X0. 03O nanoparticles (X= Mn, Ni, and Co) using Scherrer and sizestrain plot methods. *Solid State Sciences.* 2012; 14(4): 488-494.
 11. Saidani T, Zaabat M, Aida MS, Boudine B. Effect of copper doping on the photocatalytic activity of ZnO thin films prepared by sol-gel method. *Superlattices Microstruct.* 2015; 88: 315-322.
 12. Feng W, Huang P, Wang B, Wang C, Wang W, Wang T, Chen S, Lv R, Qin Y, Ma J. Solvothermal synthesis of ZnO with different morphologies in dimethylacetamide media. *Ceram Int.* 2016; 42(2, Part A): 2250-2256.
 13. Razali R, Zak AK, Majid WA, Darroudi M. Solvothermal synthesis of microsphere ZnO nanostructures in DEA media. *Ceram Int.* 2011; 37(8): 3657-3663.
 14. Suntako R. Effect of synthesized ZnO nanograins using a precipitation method for the enhanced cushion rubber properties. *Mater Lett.* 2015; 158: 399-402.
 15. Zak AK, Wang H, Yousefi R, Golsheikh AM, Ren Z. Sonochemical synthesis of hierarchical ZnO nanostructures. *Ultrason Sonochem.* 2013; 20(1): 395-400.
 16. Yousefi R, Jamali-Sheini F, Zak AK. A comparative study of the properties of ZnO nano/microstructures grown using two types of thermal evaporation set-up conditions. *Chem Vap Deposition.* 2012; 18(7-9): 215-220.
 17. Xu X, Zhou M. Antimicrobial gelatin nanofibers containing silver nanoparticles. *Fibers and polymers.* 2008; 9(6): 685-690.
 18. Ahmed F, Arshi N, Dwivedi S, Koo BH, Azam A, Alsharaeh E. Low temperature growth of ZnO nanotubes for fluorescence quenching detection of DNA. *J Mater Sci Mater Med.* 2016; 27(12): 189.
 19. Nair S, Sasidharan A, Divya Rani VV, Menon D, Nair S, Manzoor K, Raina S. Role of size scale of ZnO nanoparticles and microparticles on toxicity toward bacteria and osteoblast cancer cells. *J Mater Sci Mater Med.* 2008; 20(1): 235.
 20. Ohira T, Yamamoto O, Iida Y, Nakagawa Z-e. Antibacterial activity of ZnO powder with crystallographic orientation. *J Mater Sci Mater Med.* 2008; 19(3): 1407-1412.
 21. Wang S, Wu J, Yang H, Liu X, Huang Q, Lu Z. Antibacterial activity and mechanism of Ag/ZnO nanocomposite against anaerobic oral pathogen *Streptococcus mutans*. *J Mater Sci Mater Med.* 2017; 28(1): 23.
 22. Park S, Lee YK, Jung M, Kim KH, Chung N, Ahn E-K, Lim Y, Lee K-H. Cellular toxicity of various inhalable metal nanoparticles on human alveolar epithelial cells. *Inhal Toxicol.* 2007; 19(sup1): 59-65.
 23. Soto KF, Carrasco A, Powell TG, Murr LE, Garza KM. Biological effects of nanoparticulate materials. *Materials Science and Engineering: C.* 2006; 26(8): 1421-1427.
 24. Nie L, Gao L, Feng P, Zhang J, Fu X, Liu Y, Yan X, Wang T. Three-Dimensional Functionalized Tetrapod-like ZnO Nanostructures for Plasmid DNA Delivery. *Small.* 2006; 2(5): 621-625.
 25. Vandebriel RJ, De Jong WH. A review of mammalian toxicity of ZnO nanoparticles. *Nanotechnology, science and applications.* 2012; 5: 61.
 26. Wang L, Wang L, Ding W, Zhang F. Acute toxicity of ferric oxide and zinc oxide nanoparticles in rats. *Journal of nanoscience and nanotechnology.* 2010; 10(12): 8617-8624.
 27. Mosmann T. Rapid colorimetric assay for cellular growth and survival: Application to proliferation and cytotoxicity assays. *J Immunol Methods.* 1983; 65(1): 55-63.
 28. Darroudi M, Sabouri Z, Oskuee RK, Zak AK, Kargar H, Hamid MHNA. Green chemistry approach for the synthesis of ZnO nanopowders and their cytotoxic effects. *Ceram Int.* 2014; 40(3): 4827-4831.
 29. Baek M, Kim MK, Cho HJ, Lee JA, Yu J, Chung HE, Choi SJ. Factors influencing the cytotoxicity of zinc oxide nanoparticles: particle size and surface charge. *Journal of Physics: Conference Series.* 2011; 304(1): 012044.
 30. Hanley C, Thurber A, Hanna C, Punnoose A, Zhang J, Wingett DG. The influences of cell type and ZnO nanoparticle size on immune cell cytotoxicity and cytokine induction. *Nanoscale research letters.* 2009; 4(12): 1409-1420.
 31. Hsiao I-L, Huang Y-J. Effects of various physicochemical characteristics on the toxicities of ZnO and TiO₂ nanoparticles toward human lung epithelial cells. *Sci Total Environ.* 2011; 409(7): 1219-1228.
 32. Müller K, Kulkarni J, Motskin M, Goode A, Winship P, Skepper JN, Ryan MP, Porter AE. pH-dependent toxicity of high aspect ratio ZnO nanowires in macrophages due to intracellular dissolution. *ACS nano.* 2010; 4(11): 6767-6779.
 33. Heng BC, Zhao X, Xiong S, Ng KW, Boey FY-C, Loo JS-C. Cytotoxicity of zinc oxide (ZnO) nanoparticles is influenced by cell density and culture format. *Arch Toxicol.* 2011; 85(6): 695-704.
 34. Premanathan M, Karthikeyan K, Jeyasubramanian K, Manivannan G. Selective toxicity of ZnO nanoparticles toward Gram-positive bacteria and cancer cells by apoptosis through lipid peroxidation. *Nanomedicine: Nanotechnology, Biology and Medicine.* 2011; 7(2): 184-192.
 35. Taccola L, Raffa V, Riggio C, Vittorio O, Iorio MC, Vanacore R, Pietrabissa A, Cuschieri A. Zinc oxide nanoparticles as selective killers of proliferating cells. *Int J Nanomed.* 2011; 6: 1129-1140.
 36. Akhtar MJ, Ahamed M, Kumar S, Khan MM, Ahmad J, Alrokayan SA. Zinc oxide nanoparticles selectively induce apoptosis in human cancer cells through reactive oxygen species. *International journal of nanomedicine.* 2012; 7: 845.